Direct global measurements of tropospheric winds employing a simplified coherent laser radar using fully scalable technology and technique

Michael J. Kavaya

NASA/Marshall Space Flight Center, Code EB54, Huntsville, AL 35812 USA
michael@lidar.msfc.nasa.gov

Gary D. Spiers

Center for Applied Optics, University of Alabama, Huntsville, AL 35899 USA
garys@photon.msfc.nasa.gov

Elena S. Lobl

Hughes STX, 620 Discovery Drive, Huntsville, AL 35806 USA

Jeff Rothermel

NASA/Marshall Space Flight Center, Code ES43, Huntsville, AL 35812 USA
jeff@pcjxr.msfc.nasa.gov

Vernon W. Keller

NASA/Marshall Space Flight Center, Code PS02, Huntsville, AL 35812 USA

ABSTRACT

Innovative designs of a space-based laser remote sensing "wind machine" are presented. These designs seek compatibility with the traditionally conflicting constraints of high scientific value and low total mission cost. Mission cost is reduced by moving to smaller, lighter, more off-the-shelf instrument designs which can be accommodated on smaller launch vehicles.

1. INTRODUCTION

Measurements of tropospheric winds from space are highly desired for many NASA, NOAA, DOD, DOE, EPA, and commercial applications.[1,2] These include global climate change research, improved weather forecast accuracy, optimum aircraft routing for passenger safety/comfort and for fuel/time savings, commercial shipping storm avoidance, pollution research and regulation enforcement, and military planning. Improved weather forecasting will save lives lost to storms, as well as reduce the number of false alarms. Numerous studies have indicated that the optimum measurement approach for winds from space is a pulsed coherent laser radar (CLR)[3-5]. NASA recently completed dual Phase A and B studies, by GE Astro Space[6] and Lockheed[7], for a full tropospheric profiling instrument named the Laser Atmospheric Wind Sounder (LAWS). The studies both recommended a pulsed CO_2 laser CLR system with pulse energy near 20 J, pulse repetition frequency (PRF) near 5 Hz, optical diameter near 1.6 m, and full-time operation (100% orbit duty cycle). However, the projected mission costs were deemed unacceptable for this new era of reduced NASA resources, and the projected spacecraft resource requirements exceeded the capabilities of small satellites. NASA's Marshall Space Flight Center (MSFC) has therefore conducted an in-house effort to investigate innovative versions of LAWS which are smaller, lighter, less expensive; which consume less power, require less heat removal, fit on small spacecraft and launch vehicles; which provide valuable engineering data and space heritage; and which still deliver significant science product consistent with NASA's Mission To Planet Earth (MTPE). The working name for these instruments is Autonomous Earth Orbiting Lidar Utility Sensor (AEOLUS), after the mythical Greek god of wind. This paper reports on the progress to date of this in-house effort.

2. WHAT IS AEOLUS?

The AEOLUS project is a series of point designs of a small, lightweight, low cost, low risk instrument for measuring winds from space in regions of high aerosol backscatter. The mission goals are to:

1) provide valuable scientific information in support of NASA's MTPE,
2) demonstrate space operation of key technologies required for a full-scale LAWS,
3) implement a logical, affordable evolutionary process leading to a full-scale LAWS measurement of global tropospheric winds.

The ground rules we followed are:

1) to use components that are as close to "commercial off the shelf (COTS)" as possible,
2) to use technology and a measurement technique that is capable of scaling up to make the full-scale LAWS measurement,
3) to design a flexible instrument capable of being accommodated on a variety of platforms in space such as small satellites, the space shuttle, and space station.

The instrument design process we followed is shown in Figure 1.

3. MEASUREMENT TECHNIQUE

Both the choice of a measurement technique for AEOLUS and subsequent consideration of design trade-offs within the chosen technique have confirmed that measurement of wind from space is a complex undertaking that contains numerous and sometimes subtle interactions between:

1) the laser radar instrument parameters,
2) the available laser radar technology,
3) the capabilities of the instrument bus or carrier,
4) the launch vehicle,
5) the atmospheric target and its assumed properties.

When the various requirements of the mission that must be achieved simultaneously are considered from a system perspective, the sensor of choice for this mission is a pulsed CLR. These joint requirements include:

1) horizontal wind measurement accuracy of about 1 m/s or better,

2) sufficiently large cross-track measurement swath width for areal coverage,
3) minimal horizontal wind measurement bias,
4) horizontal wind measurement resolution of about 100 km or smaller,
5) best possible vertical resolution,
6) maximum possible allowed horizontal wind magnitude,
7) minimal prime power, cooling, and downlink data rate requirements,
8) minimal instrument mass and volume,
9) maximum mission duration,
10) eyesafe fluence exposure,
11) low mission cost.

Requirement 1 leads to the need for nearly collocated, biperspective line of sight (LOS) wind measurements. Because of spatial variability in the horizontal wind field, many LOS measurements are needed in each areal resolution element (e.g., 100 km x 100 km square) in order to reduce the contribution to error from undersampling. Since the point on the earth directly below the spacecraft moves at 7.3 km/s (350 km orbit height), the 100 km resolution requirement means that the time available for an accurate LOS horizontal wind measurement in a 100 km square is only about 14 s divided by the number of 100 km squares being probed in the cross-track direction. Using our current number of 4 cross-track squares yields about 3.5 s for each horizontal wind measurement. (The full-scale LAWS had 10 cross-track squares.) Requirement 2 means the laser beam must be scanned. The scanning may be continuous or step-stare. Continuous-scanning is preferred by the spacecraft designer who must compensate the angular momentum. Since continuous scanning involves changing the beam pointing direction with time, an accurate LOS wind measurement must occur over a short time interval due to both the varying spacecraft-earth relative velocity along the LOS, and due to the varying probe direction of the laser beam in the wind. Thus the number of laser shots per LOS measurement divided by the laser PRF must be small. Pulsed CLR satisfies this by making a measurement with as few laser shots as one. By comparison, techniques that employ many laser shots per LOS measurement, such as pulsed noncoherent laser radar (NLR), must use a high laser PRF. A higher PRF increases the required laser lifetime (in pulses), increases the on-board data processing rate, and increases the data downlink rate unless on-board combining of multiple laser shot data is performed. This is true even if the total transmitted pulse energy per LOS wind measurement is the same as CLR. To date, however, NLR measurements have proven less photon efficient than CLR, and more total energy per LOS measurement must be transmitted. The important comparisons of prime power and cooling require knowledge of each laser's efficiency. Some methods of combining laser shot data on board increase the risk of velocity bias, and preclude data processing improvements on the ground.

4. COMPONENTS OF A SPACE-BASED CLR

It was stated above that the system designer must account for the interactions of the CLR instrument, the atmospheric or earth surface target of interest, the launch vehicle, and the carrier or bus connecting the instrument to the launch vehicle. Each of these items has levels of further subdivision. A CLR broadly consists of a laser transmitter, an optics subsystem, a receiver, a control computer, a data acquisition subsystem, and a data processing computer. A simplified schematic of a CLR is shown in Figure 2. The laser subsystem consists of an optical pulse generating unit and one or two continuous-wave (CW) lasers to perform the functions of master oscillator and local oscillator (LO). The optics consist of lenses, mirrors, beamsplitters, the beam expanding telescope, the beam scanner, and, if needed, a lag angle compensation (LAC) element. The receiver comprises an optical detector, and optics to combine the received photons from the atmosphere with the LO optical field. This combination must strive to match the shape, direction, curvature, and polarization of the LO field with the expected value of signal field.

5. SPACECRAFT AND LAUNCH VEHICLE ACCOMMODATION

The spacecraft or payload of the launch vehicle consists of the carrier or bus mated to the scientific instrument(s). This payload must be accommodated by the launch vehicle in the categories of mass, volume, orbit height, orbit inclination, survivable launch vibration frequencies and amplitudes, and survivable launch accelerations. The cost of the launch vehicle and carrier must both fit in the mission budget. We are considering Pegasus XL, Conestoga, LLV, and Taurus class launch vehicles. The carrier must accommodate the needs of the instrument including electrical power, heat removal (thermal), orbit height, orbit inclination, electrical power storage in batteries, mass, data downlink rate, mechanical mating, pointing control and stability, etc.

A sun-synchronous orbit is preferred from the electrical power and heat removal viewpoints. The measurements occur over all latitudes and over all the earth after a few days. By contrast an equatorial orbit does not measure the higher latitudes, but gives more coverage of low latitudes. It receives the launch advantage of the earth's rotation, but is less desirable for electrical power and heat removal.

Lower orbit heights allow a greater payload mass, but some of this mass gain is consumed by propellent needed for additional reboosts due to increased atmospheric drag. Lower heights also provide greater SNR for fixed nadir angle, but not necessarily for fixed cross-track coverage. Atmospheric drag also depends on the sunspot cycle, which will peak from 1999 to 2004. The designs described later assume a 350 km orbit height with a 30° nadir angle which yields a 400-km wide coverage centered below the spacecraft.

The data rate is proportional to the laser PRF, the number of desired range gates (the height resolution and coverage), and the fraction of each orbit spent taking data (orbit duty cycle). The data rate may be lowered by processing data on board before transmission. Maximum science is achieved by 100% orbit duty cycle. Downlinking all data allows research into optimum velocity estimation algorithms.

Assuming a suitably located ground station with a large (~5 m) diameter S-band antenna, data can be downlinked directly from the spacecraft to the ground station at a peak data rate of ~2 Mbit/s, but only during the time the spacecraft has LOS visibility to the receiving station. This available time on any given orbit varies from zero to >5 min. with a gap between downlink opportunities sometimes as long as 20 hrs. Thus on-board data storage of several hundred Mbit may be required. A typical ground station with a small (~1 m) diameter antenna will handle only a few 10's of kbit/s. This would require use of several ground stations. At greater cost, data could be downlinked through an S-band omnidirectional antenna to the 26-m ground antenna network of the Deep Space Network (DSN), or via a geostationary communications satellite such as the Tracking and Data Relay Satellite System (TDRSS).

6. PULSED CLR DESIGN TRADES

Choosing a design point for a pulsed CLR to measure winds from space leads one to work in an onerous multi-dimensional space consisting of a dimension for each parameter of the CLR instrument, the atmospheric target, the carrier capabilities, and the launch vehicle capabilities. All of these parameters are interconnected and must be dealt with. Some of these interconnections have been previously discussed.[8] Varying one parameter to solve one problem often produces one or more new problems. Often a mean value description is inadequate and a parameter's probability distribution function (PDF) must be used (e.g., aerosol backscatter). Possible correlations among parameters must also be considered (e.g., aerosol backscatter vs. wind turbulence vs. wind shear). Some design choices are continuous (e.g., laser pulse energy, optical diameter), while others are discrete (e.g., velocity calibration with or without an earth surface return, conical scanning with a rotating telescope or a rotating wedge or a rotating flat mirror, active or passive heat removal).

An illustrative example of a design trade is the choice of design nadir angle θ, the angle between the nadir direction and the LOS laser beam direction, for a laser beam conically scanning about nadir. (All our designs assume a constant nadir angle. A variable nadir angle would increase complexity, risk, cost, and mass.) Many aspects of the system design depend on nadir angle. In some cases the dependence on nadir angle can be easily pictured, while in other cases the dependence is complex, and should be modeled on a computer. Table 1 summarizes some of the simple cases. We assume for the moment a flat earth, and do not distinguish between the nadir angle as the photons leave the CLR in space, and their nadir angle in the atmosphere. This assumption becomes more seriously incorrect as the nadir angle increases. Seeking first to maximize signal-to-noise ratio (SNR) (see case 1 in Table 1), we consider that the signal power falls inversely as the square of the slant range R. The flat earth slant range varies as $1/\cos\theta$. The noise power is proportional to the detection or search bandwidth B_S, which equals $(2/\lambda)V_S$, where V_S is the velocity search bandwidth. For a maximum design horizontal wind in any direction, V_{HM}, we find $B_S = (2/\lambda)(2V_{HM})\sin\theta$. The total SNR function is therefore $(\cos^2\theta)/\sin\theta$. The nonintuitive optimum nadir angle appears to be 0°, or straight down. However, it has been shown that SNR is not a good figure of merit (FOM) for wind velocity measurements. Picturing the detected signal in the frequency domain, the signal power is gathered in just a few, or even one, frequency bins, while the noise power, assumed white, is spread across all frequency bins. A better FOM is the ratio of the signal height to the level of the "grassy" noise, i.e., the ratio of the

total average signal energy in the observation time to the spectral density level of the noise[3,9]. This parameter Φ = SNR x M, where M is the number of data samples used to make the frequency estimate[9]. The number of data samples per estimate is proportional to both the sampling frequency of the data recorder and the observation time for one estimate. Holding the desired height resolution of the measurement constant means that the observation time goes as $1/\cos\theta$. Holding V_{HM} constant, and sampling the data stream fast enough to avoid frequency aliasing causes the sampling frequency to go as $\sin\theta$. This is case 2 in Table 1 and again yields an optimum nadir angle of 0°, but with a weaker function of θ. Next we consider that the mission goal is horizontal wind measurements and not just LOS measurements. The alignment of each LOS measurement with the horizontal wind goes as $\sin\theta$ and is shown in case 3 of Table 1. The optimum nadir angle is now 45°. This combination of LOS velocity estimation performance with horizontal alignment is heuristic and not rigorous. Two techniques of effecting a conical scan about nadir are a rotating telescope and a rotating wedge. If a wedge is used to deflect the laser beam by θ, the CLR optical diameter is reduced by the factor $\cos\theta$. This effect is added in case 4, where we specifically assume that atmospheric refractive turbulence effects are small, and that there is no transmitter/delayed back-propagated local oscillator (BPLO) misalignment angle α. The angle α occurs between the transmitted laser pulse direction and the direction of the imaginary BPLO beam as the backscattered photons reenter the CLR. The optimum nadir angle becomes 35°. We may also heuristically add the goal of large cross-track coverage by the satellite sensor. For a flat earth, we multiply by $\tan\theta$. This is included in case 5. The optimum angle becomes 55°. Case 6 assumes a rotating telescope, removes the wedge scanner, and yields that larger nadir angles are always better. We do not use the FOMs in cases 5 and 6 since the treatment of swath width is so arbitrary. Our computer simulation for estimating the performance of candidate mission designs uses a spherical earth, and also includes the more complex effects of atmospheric extinction, atmospheric refractive turbulence, and misalignment angle. Using our more sophisticated simulation for cases 4 and 5 produces the smaller optimum angles of 33° and 47°, respectively (see Figure 3). It is reasonable that addition of extinction and a spherical earth would favor smaller nadir angles. The simulation parameters correspond to our point design 5, which is discussed below. Note that we used a constant misalignment angle of 7.3 μrad, which causes a budgeted 3 dB misalignment loss at our nominal nadir angle of 30°, but varying loss at other nadir angles.

Future refinements to our FOM for just the nadir angle design trade might include the effects of nadir angle on aerosol backscatter, land backscatter, ocean backscatter, and the probability of intercepting clouds. Also related are the cost and mass of the wedge, and the effects on atmospheric shot spacing of wedge rotation rate and laser PRF.

Table 1: Selection Of Design Nadir Angle

Case	SNR $(\cos^2\theta)/\sin\theta$	Number Data Samples $\tan\theta$	Horizontal Alignment $\sin\theta$	Wedge Scanner $\cos\theta$	Cross-Track Width $\tan\theta$	Total Function	Optimum Nadir Angle (deg.)
1	✔					$(\cos^2\theta)/\sin\theta$	0
2	✔	✔				$\cos\theta$	0
3	✔	✔	✔			$\cos\theta\sin\theta$	45
4	✔	✔	✔	✔		$(\cos^2\theta)\sin\theta$	35
5	✔	✔	✔	✔	✔	$(\sin^2\theta)\cos\theta$	55
6	✔	✔	✔		✔	$\sin^2\theta$	90

The misalignment angle α is another important design trade issue, especially when selecting the laser wavelength of the CLR[8], or when selecting the optical diameter. Frehlich[10] has examined the effect of misalignment angle α on degradation of the CLR heterodyne or mixing efficiency, η_{MIX}; which is important since both SNR and Φ are proportional to it. We employ Frehlich's exact results for a circular optical aperture of diameter D, a Gaussian transmitted beam with diameter optimally matched to

D, a monostatic CLR, far field operation, and negligible refractive turbulence effects. For degradations less than 15 dB, the points approximately follow $\eta_{MIX} = 0.42 \exp[-(q/2.8)^2]$, where $q = (\pi D\alpha/\lambda)$. This is a strong function of the ratio q, which includes optical diameter, misalignment angle, and optical wavelength. If a wedge scanner is used, the diameter D refers to the smaller value exiting the wedge. For a fixed budgeted loss in SNR due to misalignment, the ratio q must be held constant. Smaller values of λ require proportionally smaller values of allowed misalignment. This is shown in Figure 4 for two wavelengths and the parameters of our point design 5. When $\alpha = 0$ and effects of refractive turbulence are negligible, the common intuition that larger values of D yield better performance is correct since SNR is proportional to receiver area = $\pi D^2/4$. However, nonzero values of α cause a reduction in this quadratic gain of performance with increasing D, and may even cause an absolute reduction in performance. This is shown in Figure 5 using the parameters of our point design 5. Even without the misalignment effect, thus having the promise of quadratic gain in performance, the optical diameter would be limited due to the penalties of mass, volume, cost, need for high optical quality, and the need to conically scan the beam. Misalignment even further reduces the optimum design diameter. We are attempting to merge the behavior of the CLR with information about realistic on-orbit misalignment angles. The actual misalignment angle will consist of contributions from prelaunch assembly and alignment of the optical subsystem, further misalignment from launch stress and orbit life, laser shot pointing jitter, and spacecraft pointing jitter during the round trip time of the transmitted photons (~ 3 ms). Techniques to eliminate the first three contributors are possible, but they complicate the instrument design.

7. INSTRUMENT DESIGNS

The NASA/MSFC AEOLUS team has nearly completed five instrument point designs. We are carrying two candidate laser technologies, the CO_2 laser at 9.11 μm wavelength, and the Tm,Ho:YLF diode-pumped solid-state laser at 2.06 μm. From our nearly COTS ground rule, and our desire for smallsat capability, we have permitted maximum laser pulse energies of 400 and 200 mJ, respectively, and a maximum optical diameter of 50 cm. Each design is examined from the mechanical, electrical, thermal, optical, laser, CLR wind measurement performance, and spacecraft accommodation perspectives. An example of CLR performance prediction for our point design number 5 is shown in Figure 6. Five curves are plotted against the atmospheric aerosol backscatter coefficient. The reflectances of land and water may also be converted into these backscatter units. This description permits scientists to determine the applicability of each CLR to measure winds of various atmospheric targets such as clear air, clouds, dust, boundary layer air, jet streams, etc. From top to bottom, the five curves are SNR_M, the unrealistic limiting case of matched filter SNR, SNR_S, the more realistic SNR calculated from the noise admitted into the velocity search bandwidth, Φ, as discussed earlier. P_g, the probability that a LOS wind estimate is "good", and σ_V, the standard deviation or spread of the "good" wind estimates[9]. The good wind estimates are clustered around the true value of the wind speed, while the "bad" estimates are uniformly distributed over a region of width V_S. All the values of σ_V are sufficiently small to provide excellent performance. Even as P_g falls to 20% for low values of backscatter, σ_V remains smaller than 0.4 m/s. Therefore, the key performance criterion to monitor is P_g. Since the backscatter value that yields $P_g = 0.5$ occurs near $\beta(2.06\ \mu m) = 2.5 \times 10^{-6}\ m^{-1}sr^{-1}$, we refer to that number as the aerosol backscatter sensitivity of design 5. As can be seen, lower values of $\beta(2.06\ \mu m)$ will produce fewer but usable velocity estimates. Note that $SNR_M \sim 3$ dB, $SNR_S \sim -15$ dB, $\Phi \sim 6$, and $\sigma_V \sim 0.3$ m/s.

All five of our point designs are contrasted in Table 2. The top row shows the backscatter sensitivity of each design. Care must be taken when comparing these values at different optical wavelengths, since backscatter varies with wavelength. Common to all 5 designs are an SNR margin of 3 dB, a budgeted misalignment loss of 3 dB, a sun-synchronous orbit height of 350 km, a 30° nadir angle, a target altitude of 300 m, transmit and receive optics efficiencies of 0.9 each, and no polarization mismatch loss. Figure 7 contrasts the sizes of designs 1-5 with the Lockheed LAWS Phase B design[7]. Design 5 has a pulse energy-receiver aperture product 15 dB below designs 3-4 in order to be accommodated on a Pegasus rocket. It achieves considerable volume and mass savings. The orbit average electrical power needed by design 5 is higher than 3-4 due to the increase of orbit duty cycle to 30% (a factor of 6), and an increase in laser PRF to 50 Hz (a factor of 5). Designs 2,4, and 5 use a rotating wedge to create a conical scan about the nadir direction. Designs 1 and 3 have two fixed pointing directions, fore and aft, to allow biperspective wind measurements along a line parallel to the ground track, but offset by 144 km. The two views of a single point in the atmosphere would be accomplished by switching the CLR between two 50 cm telescopes, and would occur about 40 s apart. This configuration has less

science value than the conical scan. Comparing the 9.11 μm designs 1-2 with the 2.06 μm designs 3-4, the cost of scanning in mass and power, as well as its lower volume can be seen.

No attempt has been made to have equal science value between the point designs at 2.06 and 9.11 μm. A study is underway to quantify the ratio of backscatter values between the two wavelengths for various candidate atmospheric targets within the sensitivity range of our different point designs. Note also that holding the misalignment loss fixed at 3 dB causes the misalignment angle specification to become stricter at 2.06 μm. Our designs are not yet mature enough to quantify the effect this stricter specification might have on instrument mass, volume, complexity, and cost; or on the suitability of candidate spacecraft.

8. CONCLUSIONS

Global tropospheric wind measurements are highly desired and will provide many benefits. Numerous studies have selected coherent laser radar as the optimum technique. Atmospheric winds have been successfully measured with coherent laser radar since 1967. A full-scale mission which measures the lowest levels of aerosol backscatter is not practical in today's economic climate. However, significant scientific benefits are possible with a smaller and more affordable instrument. Significant benefit could result in only a few years by starting a faster, smaller, cheaper mission now. NASA/MSFC is ready to design and perform such a mission. The mission will provide exciting science and will also provide valuable information for a future full-scale effort.

9. ACKNOWLEDGMENTS

The AEOLUS project was conceived by J. W. Bilbro of NASA/MSFC. The authors appreciate the suggestions of R. G. Beranek, D. B. Bowdle, R. G. Frehlich, and R. J. Koczor; and the design work of F. Amzajerdian, J. A. Dunkin, R. Eng, J. C. Fikes, P. L. Hunt, J. Jackson, S. C. Johnson, J. W. Redmon, Jr., W. A. Till, and S. P. Tucker. One of us (GDS) gratefully acknowledges the support of Dr. Ramesh K. Kakar, NASA Headquarters, under contract NAS8-38609.

10. REFERENCES

1. W. E. Baker, "Why We Need LAWS," Storm, The World Weather Magazine 1(1), 26-30, 1993.
2. R. Sadourny, "Importance of global Doppler lidar wind profiles from space for climate and environment studies," paper TuA1, p. 91, Tech. Digest of the 7th Conference on Coherent Laser Radar Applications and Technology, Paris, France, 19-23 July 1993.
3. R. T. Menzies, "Doppler lidar atmospheric wind sensors: a comparative performance evaluation for global measurement applications from earth orbit," Appl. Opt. 25(15), 2546-2553, 1986.
4. "Laser Atmospheric Wind Sounder (LAWS) Earth Observing System Instrument Panel Report," Vol. IIg, National Aeronautics and Space Administration, R. J. Curran, Chairman, Jan. 1987.
5. R. G. Beranek et al, "Laser Atmospheric Wind Sounder (LAWS)," Proc. SPIE 1062, 234-248, 1989.
6. "Definition and Preliminary Design of the Laser Atmospheric Wind Sounder (LAWS)." Phase II Final Report, NASA Contract NAS8-37589, Volume I, Executive Summary and Volume II, Final Report, GE Astro Space, 9/30/92.
7. "Design Definition of the Laser Atmospheric Wind Sounder (LAWS)," Phase II Final Report, DR-20, NASA Contract NAS8-37590, Volume I, Executive Summary, June 1992, and Volume II, Final Report, November 1992, Lockheed Missiles & Space Company.
8. M. J. Kavaya, "Wavelength trade considerations for space-based coherent lidar measurement of winds," paper MD3, p. 78, Tech. Digest of the 7th Conference on Coherent Laser Radar Applications and Technology, Paris, France, 19-23 July 1993.
9. R. G. Frehlich and M. J. Yadlowsky, "Performance of Mean-Frequency Estimators for Doppler Radar/Lidar," to be published in J. Atmospheric and Oceanic Technology, 1994.
10. R. G. Frehlich, "Heterodyne efficiency for a coherent laser radar with diffuse of aerosol targets," submitted to J. Modern Optics, 1993.

DESIGN PARAMETER	NO. 1	NO. 2	NO. 3	NO. 4	NO. 5A THIN CLOUDS	NO. 5B THICK CLOUDS
PERFORMANCE						
BACKSCATTER(/M-SR)@50%	8.2E-09	1.1E-08	5.7E-08	7.6E-08	2.5E-06	3.9E-05
SNR MARGIN, dB	3	3	3	3	3	3
VERTICAL RESOLUTION, M	1000	1000	1000	1000	1000	64
MAXIMUM HORIZONTAL WIND, M/S	30	30	30	30	50	50
INSTRUMENT						
LASER WAVELENGTH, μM	9.11	9.11	2.06	2.06	2.06	2.06
SCAN TYPE	dual-look	scan wedge	dual-look	scan wedge	scan wedge	scan wedge
PULSE ENERGY, mJ	400	400	200	200	25	25
PRF, Hz	20	20	10	10	50	50
TELESCOPE DIAMETER, M	0.5	0.5	0.5	0.5	0.25	0.25
MISALIGNMENT LOSS, dB	3	3	3	3	3	3
MISALIGNMENT ANGLE, μRAD	13.9	16.1	3.15	3.64	7.28	7.28
SIZE, M	1.22x1.24x1.33	1.22(D)x1.35	1.22x1.24x1.33	1.22(D)x1.35	0.73(D)x0.99	0.73(D)x0.99
Inches	48.0x48.8x52.4	48.0(D)x53.3	48.0x48.8x52.4	48.0(D)x53.3	28.8(D)x38.9	28.8(D)x38.9
VOLUME, M3	2	1.6	2	1.6	0.4	0.4
ft3	71	55.8	71	55.8	14.7	14.7
MASS, Kg	231	266	191	226	125	125
lbs	508	585	420	497	275	275
POWER, W (STBY/WARM-UP/OPER)	160/332/437	168/378/476	75/182/355	83/226/391	83/221/331	83/221/331
ORBIT DUTY CYCLE, %	5	5	5	5	30	30
ORBIT AVERAGE POWER, W	203	219	107	122	180	180

Table 2 AEOLUS designs intercomparison.

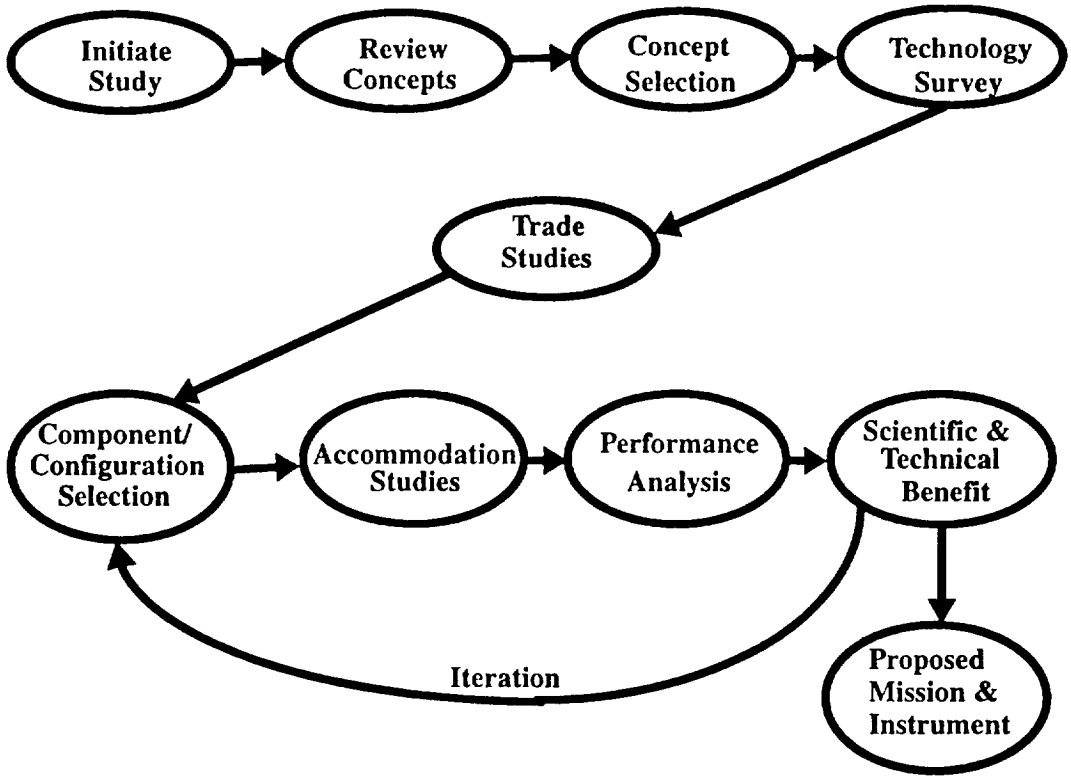

Figure 1 AEOLUS instrument design process.

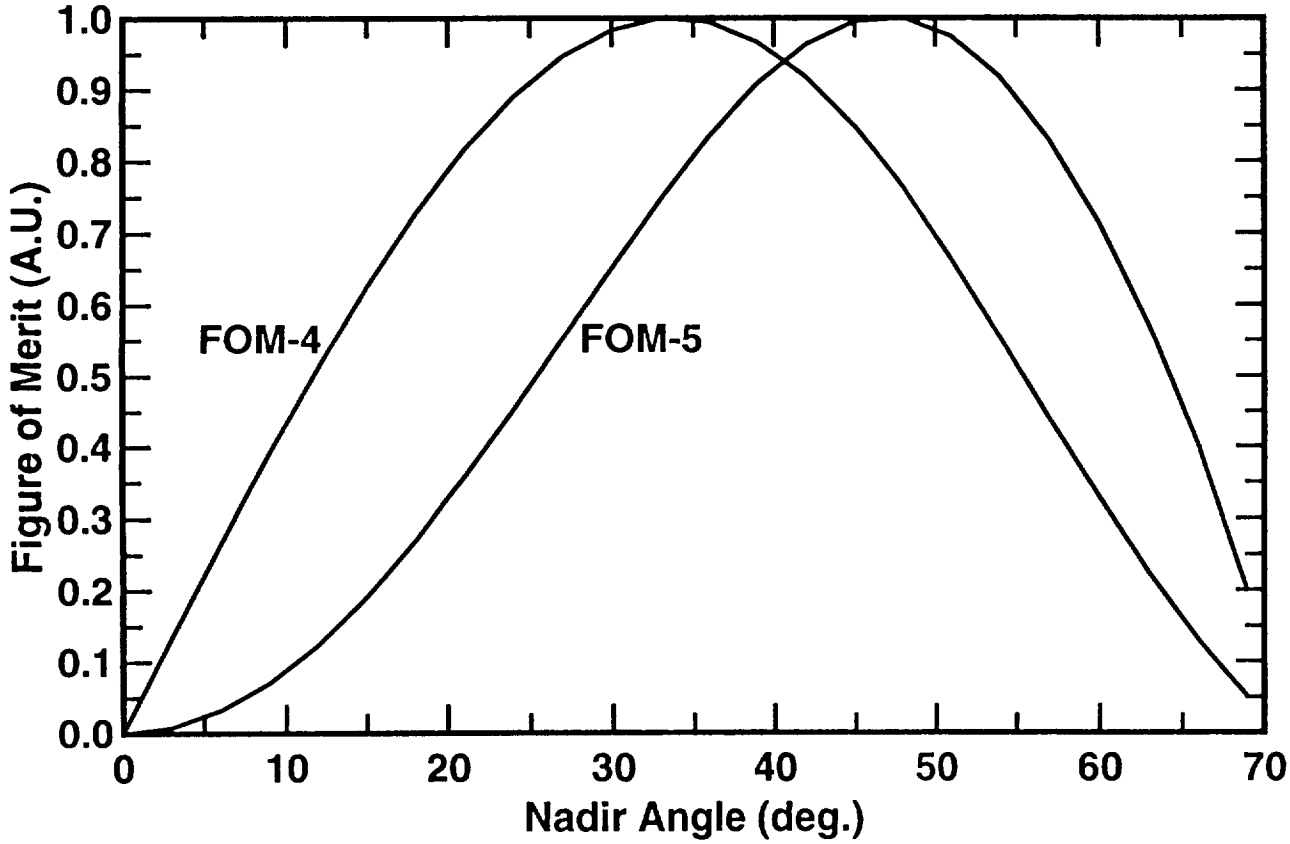

Figure 3 Two selected figures of merit as a function of nadir angle (see text).

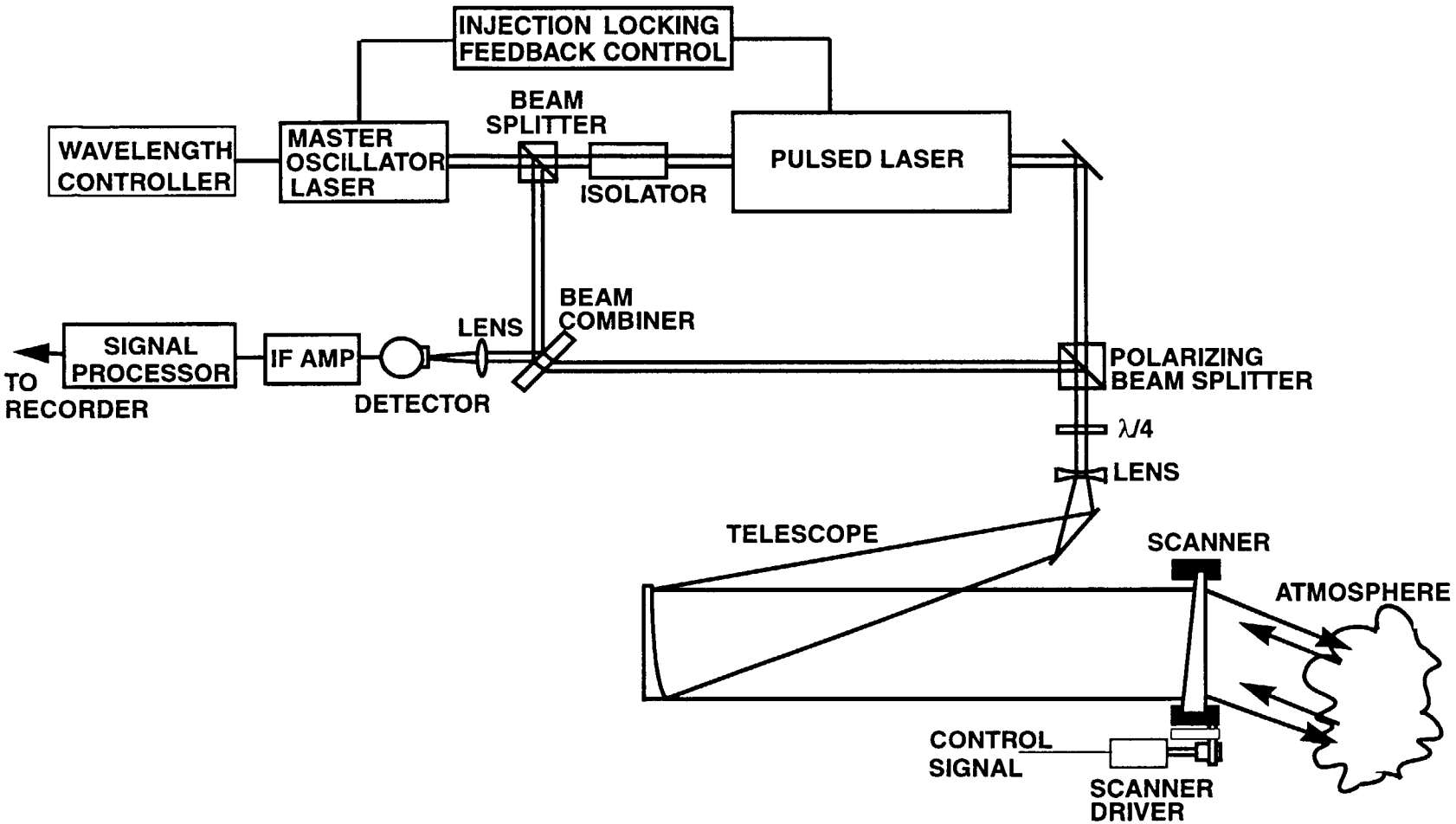

Figure 2 Optical Schematic for AEOLUS point design no. 5.

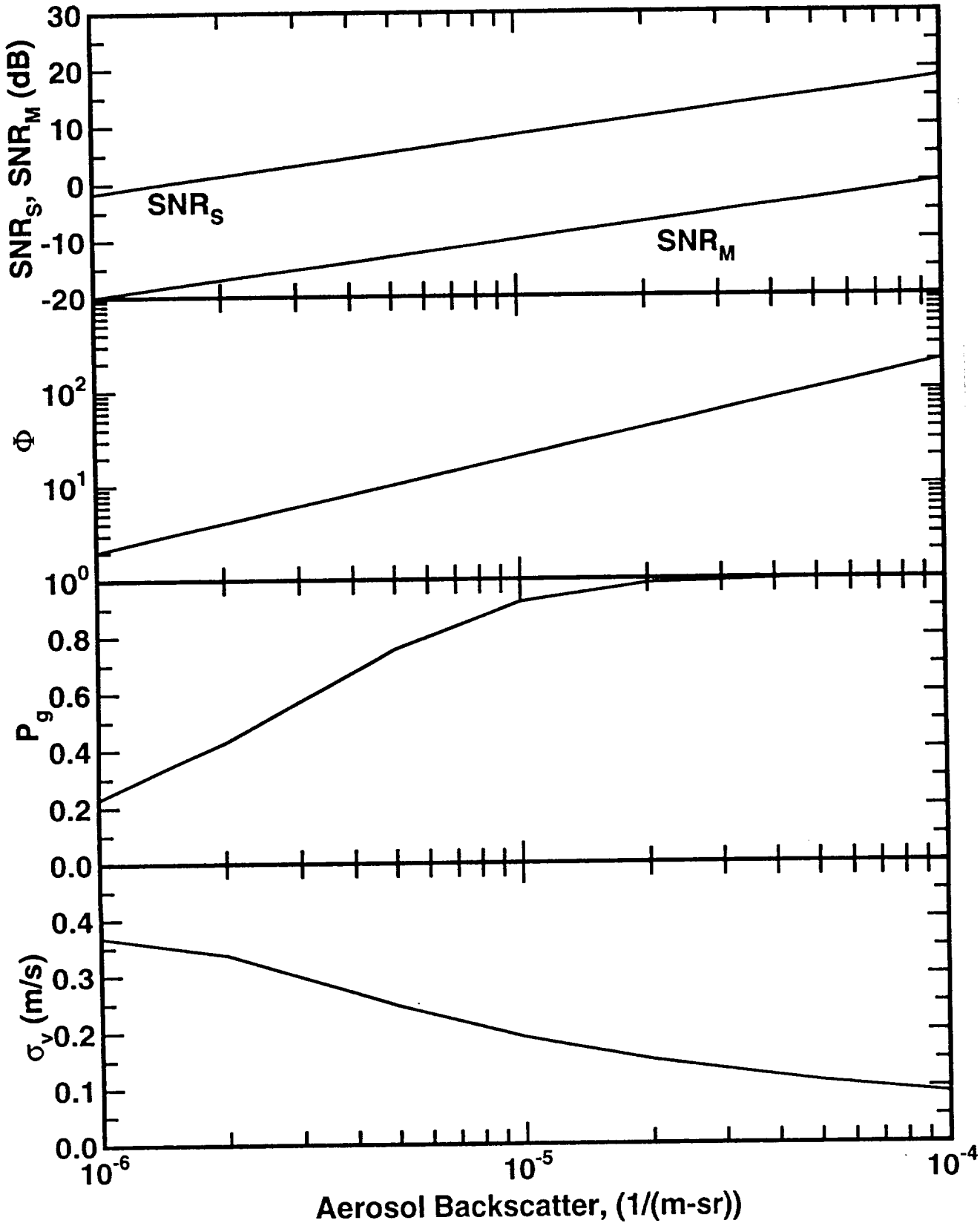

Figure 6 A representative performance analysis for Design No. 5 with a 1 km vertical integration range.

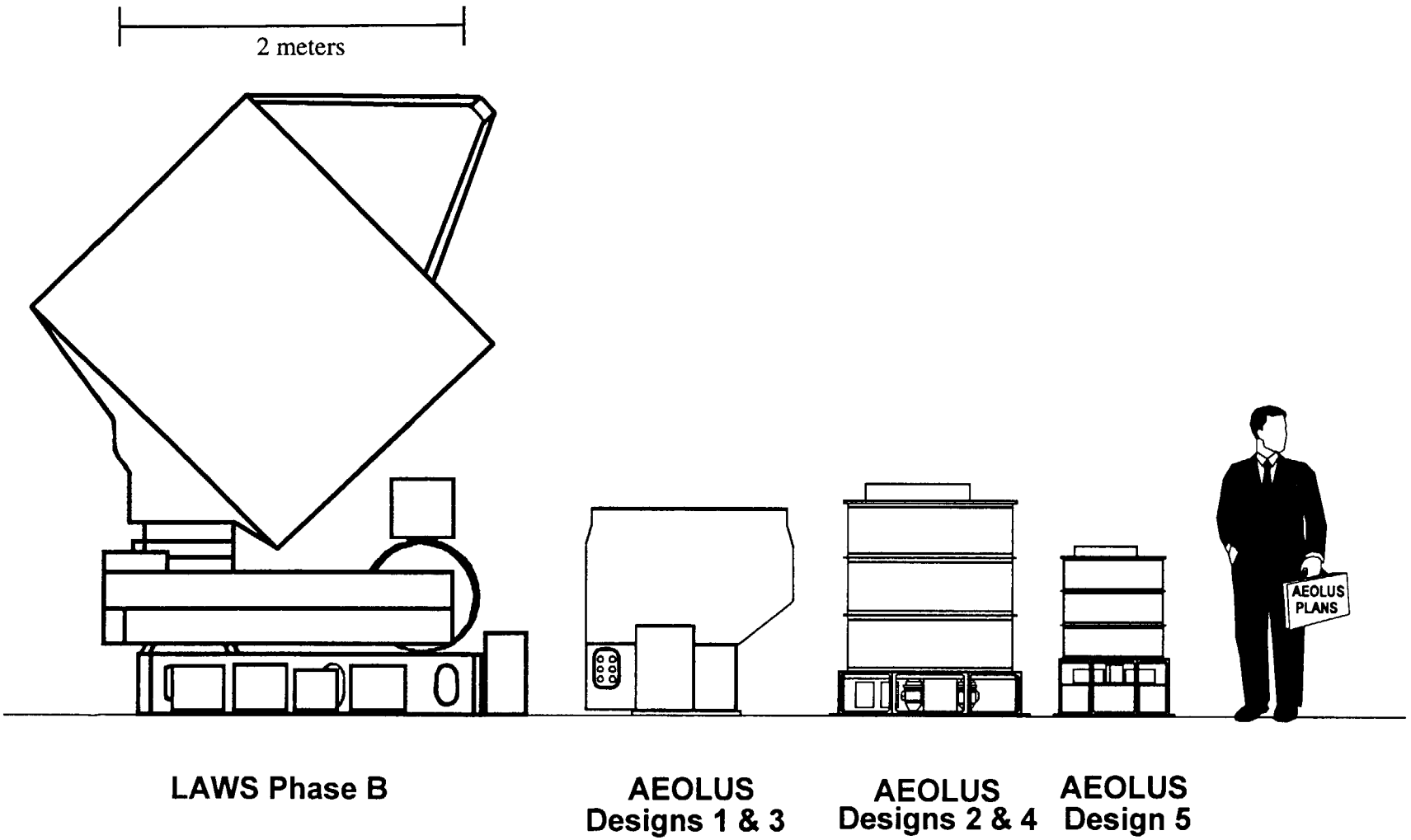

Figure 7 Comparison of AEOLUS designs and one of the LAWS Phase B designs.